RSC Advances

ROYAL SOCIETY OF CHEMISTRY

www.rsc.org/advances

Significant enhancement of the upconversion emission intensity of Y_2O_2S: Er^{3+} was achieved by Mn^{2+} sensitizing under 1550 nm excitation.

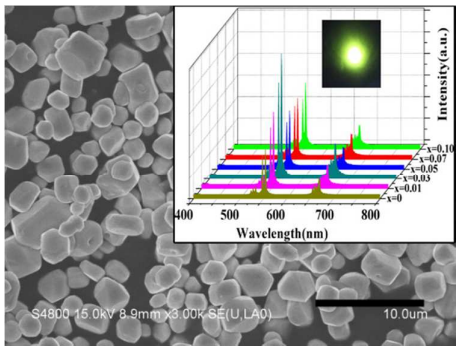

Significant Enhancement of Visible Up-conversion Emissions of $Y_2O_2S:Er^{3+}$ Phosphors by Mn^{2+} Sensitizing Under 1550 nm Excitation

Shuanglong Yuan,[a] Huidan Zeng,[a,*] Xuanshun Wu,[a] Zhao Liu,[a,b] Jing Ren,[a] Guorong Chen,[a] Zhaofeng Wang,[c] Luyi Sun,[c,*]

[a]Key Laboratory for Ultrafine Materials of Ministry of Education, School of Materials Science and Engineering, East China University of Science and Technology, Shanghai 200237, China

[b]State Key Laboratory of Luminescent Materials and Devices, South China University of Technology, Guangzhou, 510640, China

[c]Department of Chemical & Biomolecular Engineering and Polymer Program, Institute of Materials Science, University of Connecticut, Storrs, Connecticut 06269, United States

*Authors to whom correspondence should be addressed.

Dr. Huidan Zeng, Tel: 86-21-64253395; Fax: 86-21-64253395; E-mail: hdzeng@ecust.edu.cn

Dr. Luyi Sun, Tel: (860) 486-6895; Fax: (860) 486-4745; Email: luyi.sun@uconn.edu

Abstract

A novel up-conversion (UC) emission route of Er^{3+} by Mn^{2+} sensitizing in $Y_2O_2S:Er^{3+}$ phosphor prepared via a high-temperature solid-state reaction method is reported here. This methodology resulted in a significant enhancement of visible up-conversion emission by a 1550 nm laser diode excitation. By co-doping Mn^{2+}, the visible (red and green) UC emission intensity, which is assigned to the transitions of $^4F_{9/2}\rightarrow{}^4I_{15/2}$ (670 nm), $^4S_{3/2}\rightarrow{}^4I_{15/2}$ (547 nm), $^2H_{11/2}\rightarrow{}^4I_{15/2}$ (528 nm) of Er^{3+}, was 2 to 3 times higher than that of the Mn^{2+}-free one. As the concentration of Mn^{2+} was increased, the visible UC emission intensity was enhanced and then reduced. The phosphor powders were well crystallized in a hexagonal shape with an average size of ca. 2 μm. Based on the results of the luminescence spectra, energy matching conditions and three-photon process dependence on excitation power, possible UC mechanism is proposed. The proposed sensitizing route may lead to a promising step towards high-intensity UC emissions of rare-earth ions doped phosphors.

Keywords: Up-conversion; 1550 nm excitation; Er^{3+}, Mn^{2+} co-doped Y_2O_2S

Introduction

The lanthanide infrared (IR)-to-visible up-conversion (UC) phenomenon has attracted high attention for its potential applications in IR pumped imaging, bio-imaging, displays, lasers, and solar cells.[1-3] With the advent of low cost, readily available and powerful IR laser diodes, there has been a renewed interest in UC. Notably, the trivalent Er^{3+} ions are considered the potential up-convertors for red, green, and blue emissions because of their rich energy levels, which well fit the excitation of commercial IR laser diodes. However, Er^{3+} ions doped samples usually exhibit low UC emission intensity when excited by the lights in the range of 1000-1600 nm, which strongly limits the application and development of these UC phosphors in the infrared wavelength region. Yb^{3+} ions have been virtually exclusively used as a trivalent rare earth sensitizer at the 980 nm excitation, but they are not effective in the 1000-1600 nm excitation range.[4-6] In particular, Yb^{3+} ions perform poorly when excited by a commercial 1550 nm laser diode, which is one of the most widely used laser diodes on market currently. In order to improve the UC emission intensity at the 1550 nm excitation, we must seek alternative efficient sensitizers.

Non-rare-earth ions, which exhibit excellent performance, have been frequently used as co-dopants to improve the phosphor optical properties.[7-9] As reported in the literature,[10-14] UC of rare earth (RE)-transition metal (TM) ions co-doping system benefits from the combined advantages of specific energy levels of RE ions and tunable energy levels of TM ions, which are very attractive for a wide range of applications.[15-17] The choice of different hosts and RE/TM dopants may result in

novel and desirable UC properties.[18]

TM ions have been widely used in luminescent materials. Among them, Mn^{2+}, as a typical luminescent center, has attracted high interest for various applications because of its unique optical properties.[19-24] Mn^{2+} has been studied in various inorganic hosts covering a wide emission range from blue to red.[25] Recently, green UC emission of Mn^{2+} at room temperature was observed in non-halide material $LaMgAl_{11}O_{19}$: Yb^{3+}, Mn^{2+}.[15, 17] The UC luminescence of the Er^{3+}/Mn^{2+} pair was extensively investigated in $Yb_3Al_5O_{12}$ at low temperatures under IR laser excitation.[26] Compared to other host matrices (e.g., chalcogenides, fluorides, oxides), the commercial phosphor host Y_2O_2S exhibits favorable chemical stability as well as higher luminescent efficiency due to its moderate phonon energies (about 520 cm^{-1}), wide band gap, and high energy transfer efficiency.[27] Thus, Y_2O_2S is expected to exhibit UC when co-doped with Er^{3+} and Mn^{2+} due to the crystal local field.

In this work, Er^{3+}/Mn^{2+} co-doped Y_2O_2S phosphors were prepared, with an aim to develop a novel route that can significantly enhance the visible UC emission intensity by the 1550 nm excitation. To the best of our knowledge, this is the first report on the 1550 nm excited UC spectral studies in Er^{3+}/Mn^{2+} co-doped Y_2O_2S phosphors.

Experimental

Sample preparation

The phosphors were prepared by the high-temperature solid-state reaction method. Stoichiometric amounts of starting materials Y_2O_3 (99.99%), Er_2O_3 (99.99%) and S

(99.999%), $MnCO_3$ (analytical grade) and Na_2CO_3 (analytical grade) were thoroughly mixed in an agate mortar. The concentrations of these rare earth oxides and $MnCO_3$ were formulated according to the chemical formula of $(Y_{0.95-x},Er_{0.05},Mn_x)_2O_2S$ (x=0, 0.01, 0.03, 0.05, 0.07, 0.10) and $(Y_{0.97},Mn_{0.03})O_2S$ (denoted as YM1). The Na_2CO_3 acted as a flux for the sintering process. The pre-determined amount of the starting materials were mixed, and sintered at 1100 °C for 3 h using an alumina crucible with an alumina cover in carbon reducing atmosphere,[28] and then cooled down to room temperature in the furnace. The sintered samples were further treated by washing with dilute hydrochloric acid (pH≈1) and distilled water several times. The washed powders were subsequently filtered and dried. The resultant fine powders were collected for characterization.

Characterization

The phosphor samples were characterized by X-ray diffraction (XRD) (Rigaku, D/Max-RB, Cu K_α radiation, λ=0.15406 nm). Electron paramagnetic resonance (EPR) spectra of the samples were recorded on a Bruker EMX-8/2.7 EPR spectrometer operating in the X-band frequency (9.877 GHz). The morphology of the phosphor samples was examined by a field emission scanning electron microscope (FE-SEM, S-4800, Hitachi High-Technologies). Absorption spectra of the samples were acquired on a UV-Vis-NIR spectrophotometer (CARY 500, Varian Company). The UC luminescence spectra were recorded at room temperature on an Edinburgh FLS920P spectrometer, excited by a tunable 1550 nm semiconductor laser diode (0-500 mW).

Results and discussion

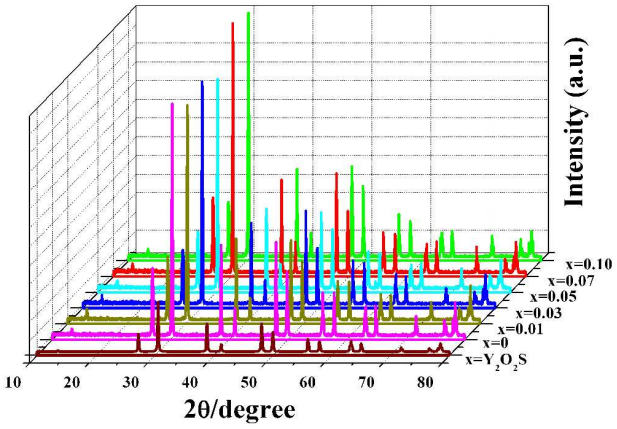

Figure 1. XRD patterns of $(Y_{0.95-x})_2O_2S$: $Er_{0.1,}Mn_x$ (x=0, 0.01, 0.03, 0.05, 0.07, 0.10) samples and standard Y_2O_2S crystal.

The XRD patterns of the as-synthesized samples with various Mn^{2+} ions concentrations are shown in Figure 1. According to the XRD patterns, the phases of all samples are hexagonal Y_2O_2S (JCPDS # 24-1424) without any detectable impurity, which suggests that the crystalline hexagonal phase of Y_2O_2S samples were obtained by the high-temperature solid-state reaction method and their structural morphology was not influenced by the addition of Mn^{2+} ions. Figure 1 also shows that the Mn^{2+}-doping approach does not result in phase transformation, but the 2θ values of the XRD peaks for all Er/Mn co-doped samples are slightly lower than those of typical hexagonal Y_2O_2S. Y_2O_2S crystallizes in space group P_{-3m1}(164) with the metal ions at the Wyckoff site 2d with 3m (C_{3v}) point group symmetry, surrounded by four oxygen and three sulfur ions.[29] The calculated cell parameters (*a, b, c*) (listed in Table

1) of the samples become slightly larger, indicating that the Mn^{2+}-doped ions have a weak influence on the host crystal lattice.

Table 1. The unit cell parameters of the samples $(Y_{0.95-x},Er_{0.05},Mn_x)_2O_2S$ (x=0, 0.01, 0.03, 0.05, 0.07, 0.10) compared with the standard trigonal Y_2O_2S.

Sample No.	Formula	Unit cell parameters		
		a/ Å	b/ Å	c/ Å
Reference	Y_2O_2S	3.785	3.785	6.571
YEM0	$(Y_{0.95},Er_{0.05})_2O_2S$	3.789	3.789	6.609
YEM1	$(Y_{0.95-x},Er_{0.05},Mn_{0.01})_2O_2S$	3.799	3.799	6.616
YEM2	$(Y_{0.95-x},Er_{0.05},Mn_{0.03})_2O_2S$	3.806	3.806	6.621
YEM3	$(Y_{0.95-x},Er_{0.05},Mn_{0.05})_2O_2S$	3.812	3.812	6.625
YEM4	$(Y_{0.95-x},Er_{0.05},Mn_{0.07})_2O_2S$	3.817	3.817	6.627
YEM5	$(Y_{0.95-x},Er_{0.05},Mn_{0.10})_2O_2S$	3.824	3.824	6.628

Generally, there are two possible sites for the doped Mn^{2+}: the interstices or the sites of Y^{3+} (the radius difference is less than 30%).[30] From the increase of the cell parameters (*a, b, c*) as shown in Table 1, one can conclude that the occupy sites should be the interstices because the ionic size of Mn^{2+} is significantly smaller than that of Y^{3+}. This is also consistent with a recent report by Yang et al.,[31] which suggested that Mn^{2+} could partially enter interstitial sites when Mn^{2+} cations were doped into $SrTiO_3$ due to the relatively large difference in ionic radius between Sr^{2+} and Mn^{2+}. To compensate the charge of Mn^{2+} in the interstitial sites, some O^{2-} or S^{2-} should also exist there. Hence, luminescence defects will be produced during the interstitial process of Mn^{2+} (assigned as $I_{(Mn)}$).[32, 33] These defects would introduce some new energy levels in the energy band of Y_2O_2S host matrix, which has

significant influence on the photoluminescence properties of the phosphors.[34, 35]

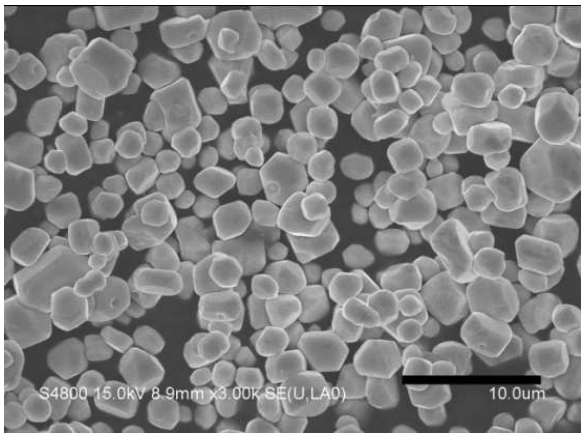

Figure 2. SEM image of $(Y_{0.92}Er_{0.05}Mn_{0.03})_2O_2S$ sample.

The prepared samples with various Mn^{2+} concentrations exhibit similar particle size and size distribution. Figure 2 shows a representative SEM image of the as-fabricated $(Y_{0.92}Er_{0.05}Mn_{0.03})_2O_2S$ sample. The sample is of hexagonal morphology with smooth surface and an average grain size is ca. 2 μm.

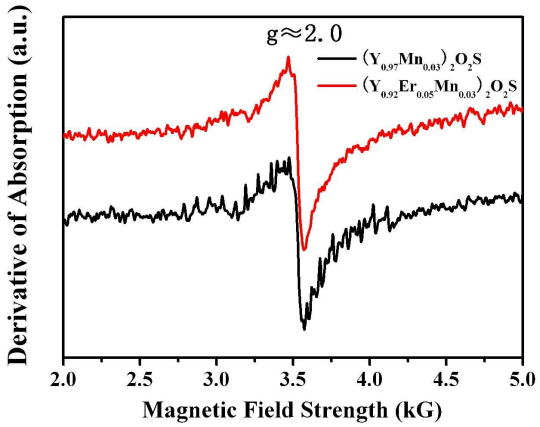

Figure 3. EPR spectra of $(Y_{0.92}Er_{0.05}Mn_{0.03})_2O_2S$ and $(Y_{0.97}Mn_{0.03})_2O_2S$ samples.

EPR was further utilized to determine the existence of Mn^{2+}. Figure 3 presents the EPR spectra of $(Y_{0.95-x},Er_{0.05},Mn_{0.03})_2O_2S$ and $(Y_{0.94},Mn_{0.03})_2O_2S$ samples. The resonance signals at a g value of ca. 2.0 were observed, in good agreement with the characteristic electron spin *S* and nuclear spin *I* of Mn^{2+} (S=I=5/2).[36] Therefore, the EPR results support that Mn^{2+} ions have been successfully doped into the Y_2O_2S host lattice.

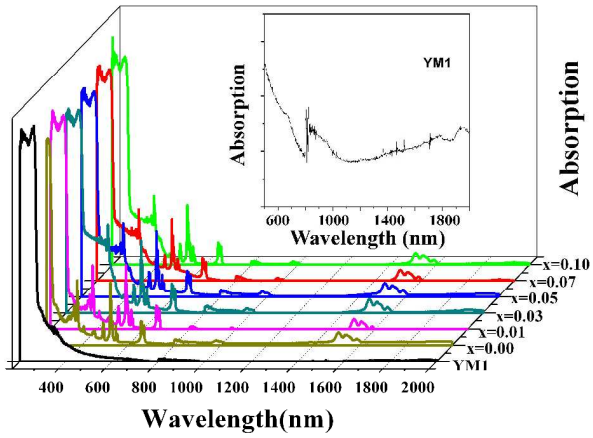

Figure 4. Absorption spectra of $(Y_{0.95-x}Er_{0.05}Mn_x)_2O_2S$ (x=0, 1.0, 3.0, 5.0, 7.0, 10.0 mol%).

The absorption spectra of the samples with various Mn^{2+} concentrations are shown in Figure 4, from which several absorption bands of Er^{3+} in all Er or Er/Mn co-doped samples can be observed. These absorption bands can be attributed to the transitions of $^4I_{15/2}\rightarrow {}^4G_{11/4}$ (381 nm), $^4I_{15/2}\rightarrow {}^4F_{7/2}$ (495 nm), $^4I_{15/2}\rightarrow {}^2H_{11/2}$ (524 nm), $^4I_{15/2}\rightarrow {}^4F_{9/2}$(661 nm), $^4I_{15/2}\rightarrow {}^4I_{9/2}$ (808 nm), $^4I_{15/2}\rightarrow {}^4I_{11/2}$ (980 nm), $^4I_{15/2}\rightarrow {}^4I_{13/2}$ (1550 nm) of Er^{3+}.[37] By increasing Mn^{2+} concentration from 0 to 10.0 mol%, there was little influence on the entire absorption in the VIS-IR range. The zoomed absorption

spectrum of the Mn^{2+} single-doped sample YM1 is shown in the inset of Figure 4, from which one can observe an obvious absorption band in the range of 800 to 1000 nm wavelength. This absorption band does not match any Mn^{2+} energy level according to Tanabe-Sugano diagram for d^5 ions,[38] which suggests that the band probably originates from $I_{(Mn)}$. Moreover, such a band overlaps with the Er^{3+} doped samples.

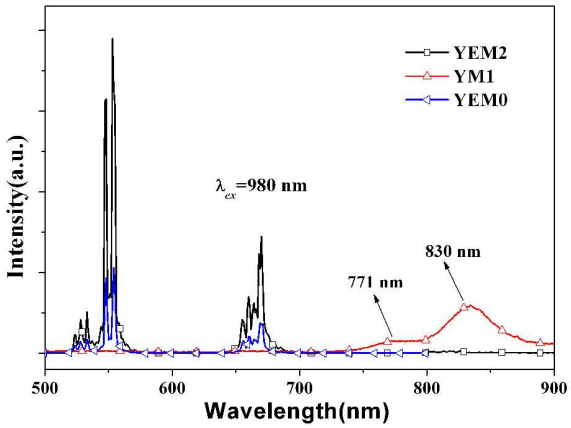

Figure 5. UC luminescence spectra of samples excited at 980 nm.

Room temperature UC luminescence spectra of $(Y_{0.97}Mn_{0.03})_2O_2S$, $(Y_{0.95}Er_{0.05})_2O_2S$ and $(Y_{0.92}Er_{0.05}Mn_{0.03})_2O_2S$ samples when excited at 980 nm are shown in Figure 5. It is interesting to note that the sample doped with Mn^{2+} only exhibited a broad non-symmetric emission band peaking at ca. 830 nm accompanied with a weak hump centered at ca. 771 nm. This is in accordance with the absorption spectrum of $(Y_{0.97}Mn_{0.03})_2O_2S$. Such broad emission band only exists in Mn^{2+} single-doped samples, but is not shown in the Er^{3+}/Mn^{2+} co-doped samples. Therefore, it is concluded that doping of Mn^{2+} would introduce a new energy level (assigned as

$E_{[Mn]}$) at ca. 830 nm. This energy level overlaps with $I_{9/2}$ level of Er^{3+}, which can potentially facilitate the energy transfer from $E_{[Mn]}$ to Er^{3+} in Er^{3+}/Mn^{2+} co-doped samples.

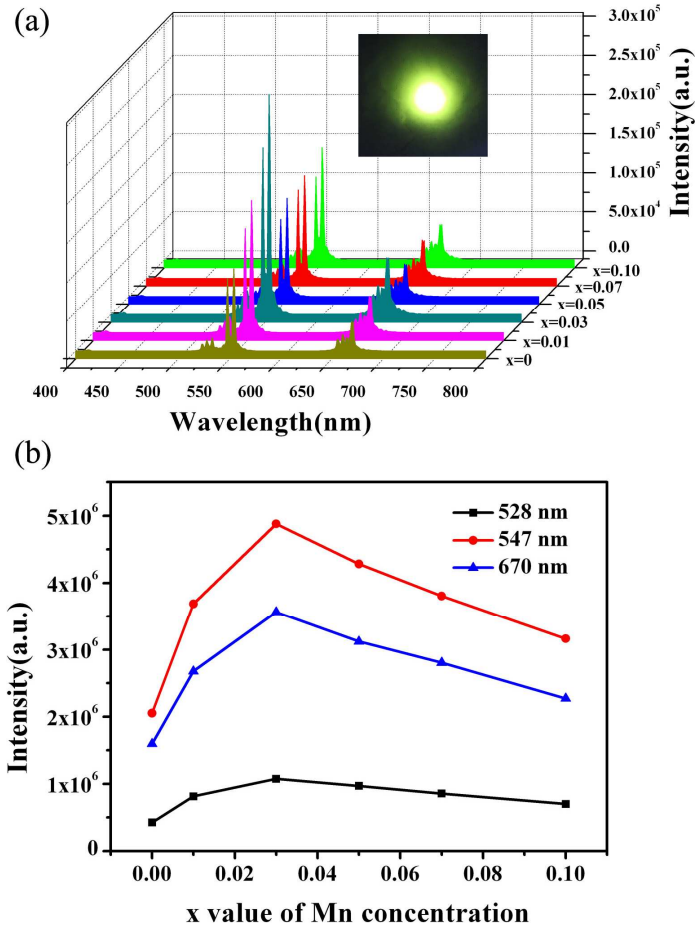

Figure 6. (a) UC luminescence spectra of $(Y_{0.95-x}Er_{0.05}Mn_x)_2O_2S$ (x=0, 1.0, 3.0, 5.0, 7.0, 10.0 mol%) samples excited at 1550 nm. The inset is a photograph of the UC emission of $(Y_{0.92}Er_{0.05}Mn_{0.03})_2O_2S$ under 50 mW excitation power. (b) Variations of UC emission (528, 548 and 670 nm) intensity as a function of Mn^{2+} concentration.

Room temperature UC luminescence spectra of the samples with various Mn^{2+} concentrations when excited at 1550 nm are shown in Figure 6. The inset show a photograph of the UC emission $(Y_{0.92}Er_{0.05}Mn_{0.03})_2O_2S$ upon 50 mW excitation at 1550 nm. In Figure 6(a), the emission spectra in the 520-680 nm range are characterized by an intense green band at ca. 547 nm followed by an intense red band at ca. 670 nm. These emissions are strong to the naked eyes. The emission bands are observed in three regions that are composed of several overlapping peaks due to the crystal-field splitting, and can be attributed to the transitions $^4F_{9/2}\rightarrow{}^4I_{15/2}$ (670 nm), $^4S_{3/2}\rightarrow{}^4I_{15/2}$ (547 nm), $^2H_{11/2}\rightarrow{}^4I_{15/2}$ (528 nm) of Er^{3+}. The sample without Mn^{2+} exhibits the lowest emission intensity among all samples. During the measurement, we also found that doping of Mn^{2+} did not result in peak shape or position evolution. And, Mn^{2+} single-doped sample $(Y_{0.97}Mn_{0.03})_2O_2S$ has no UC emission, which means that the introduced new energy level $E_{[Mn]}$ by Mn^{2+} does not match the energy of 1550 nm. In Figure 6(b), as the concentration of Mn^{2+} ions increases from 1.0 to 3.0 mol%, the emission intensity increases gradually. It is noticeable that further increasing the concentration of Mn^{2+} to 10.0 mol% remarkably decreases the intensity of both green and red emission bands. The involved mechanism will be further discussed in the following paragraphs. It should be noted that the UC emission intensity of $(Y_{0.92}Er_{0.05}Mn_{0.03})_2O_2S$ phosphor was 2-3 times as intense as $(Y_{0.95}Er_{0.05})_2O_2S$.

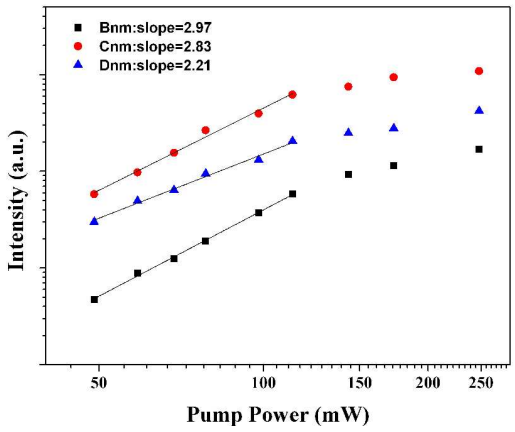

Figure 7. Log-log plot of the UC emission intensities as a function of the 1550 nm excitation power for $(Y_{0.92}Er_{0.05}Mn_{0.03})_2O_2S$ sample.

The dependence of the pumping power and luminescence intensity of $(Y_{0.92}Er_{0.05}Mn_{0.03})_2O_2S$ sample is shown in Figure 7, in which the number of photons n determined from the slope coefficient of the linear fitted lines is 2.21, 2.83, 2.97 monitored at the emission peak wavelength 670, 548 and 524 nm, respectively. This result indicates that the UC luminescence is attributed to a three-photon absorption (TPA) mechanism, which is consistent with the literature [2].

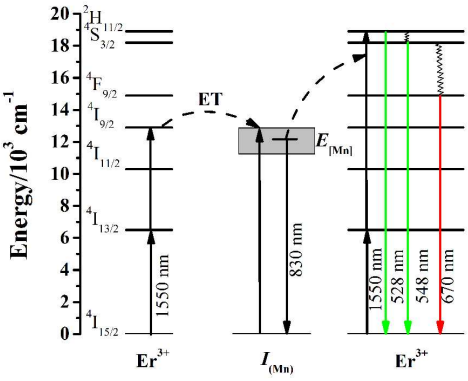

Figure 8. Proposed UC luminescence mechanism of Er^{3+}, Mn^{2+} co-doped Y_2O_2S excited at 1550 nm.

Based on the results of the luminescence spectra, the energy matching conditions, and the TPA processes, the following possible UC mechanism is proposed. Initially, Er^{3+} can be directly excited from ground state to $^4I_{13/2}$ level via the absorption of a 1550 nm photon, and it can be further excited to $^4I_{9/2}$ level by absorbing another 1550 nm photon. The electron of Er^{3+} at $^4I_{9/2}$ level can be further excited to a higher energy level ($^2H_{11/2}$), generating the emission bands at 528, 548, and 670 nm ($^2H_{11/2}\rightarrow{}^4I_{15/2}$, $^4S_{3/2} \rightarrow 4I_{15/2}$, and $^4F_{9/2} \rightarrow 4I_{15/2}$ transitions, respectively) through non-radiation relaxation. For this reason, the Er^{3+} doped sample can exhibit UC luminescence. When Mn^{2+} was co-doped in the matrix, it turned to be different because $I_{(Mn)}$ could act as an efficient sensitizing center. Since the energy of $^4I_{9/2}$ level of Er^{3+} is slightly larger than that of the $E_{[Mn]}$ level originated from $I_{(Mn)}$, the energy transfer (ET) process from Er^{3+} to $I_{(Mn)}$ dominates in the excitation of $E_{[Mn]}$ level (ca. 830 nm, which can be reflected from Figure 5). As the $E_{[Mn]}$ matches well with $^4I_{13/2}$-$^2H_{11/2}$, part of the populated $^4I_{13/2}$ level is excited to the $^2H_{11/2}$ state from the $I_{(Mn)}$ emission channel. Similar energy transfer between Er^{3+} and Mn^{2+} was also reported in a recent research.[39] After these excited state processes, de-excitation accumulates electrons in different excited states and the intensity of emission depends on the electron density at that particular level as well as the non-radiative contribution to the emission band. The level $^2H_{11/2}$ acts as a meta-stable level and the emission from $^2H_{11/2}$ to $^4I_{15/2}$ results in 528 nm emission. Since the $^2H_{11/2}$ level couples to the $^4S_{3/2}$ level by lattice phonon relaxation between closely spaced energy levels, the level $^4S_{3/2}$ act as a meta-stable

level and the emission from $^4S_{3/2}$ to $^4I_{15/2}$ results in 547 nm emission. Fractional populations accumulated in level $^4F_{9/2}$ decays to $^4I_{15/2}$, giving rise to emissions at 670 nm. In oxysulfide hosts, because of the weak lattice phonon relaxation, the non-radiative contribution to 547, 670 nm emission bands forms the energy gap between $^4S_{3/2} \leftrightarrow {}^4F_{9/2}$ (Er^{3+}).

The optimal doping concentration of Mn^{2+} is found to be 3.0 mol%, and the corresponding emission intensity is 2-3 times higher than that of $(Y_{0.95}Er_{0.05})_2O_2S$. By Mn^{2+} sensitizing in $Y_2O_2S:Er^{3+}$ phosphor, the visible UC emission intensity enhances significantly due to the increase of the photon numbers of the $^2H_{11/2}$ (Er^{3+}) level. With the further increase of Mn^{2+} ions, however, the intensity of luminescence grows less intense. Similar phenomena have been widely reported for the Mn^{2+} ions doped glasses,[40, 41] and are ascribed to the concentration quenching effect that is due to the cross-relaxation caused by the interactions of Mn^{2+} ions.

Conclusions

The 1550 nm excited UC process of Er^{3+}/Mn^{2+} co-doped Y_2O_2S phosphors prepared by a high-temperature solid-state reaction method is reported for the first time. Through Mn^{2+} ions doping, hexagonal phase of the samples remains intact, and their average size is ca. 2 μm. By co-doping Mn^{2+}, $Y_2O_2S:Er^{3+}$ samples exhibit strong green and red UC emission under the excitation of 1550 nm laser. The UC emission intensity of $(Y_{0.92}Er_{0.05}Mn_{0.03})_2O_2S$ phosphor is 2-3 times higher than that of $(Y_{0.95}Er_{0.05})_2O_2S$. It is hoped that this report will stimulate further discoveries of other

UC materials with the designed structure and desirable optical functionalities.

Acknowledgement

This work is financially supported by the Natural Science Foundation of Shanghai (12ZR1407600, 11ZR1409300), the Fundamental Research Funds for the Central Universities, the Shanghai Leading Academic Discipline Project (B502), and the Open Fund of the State Key Laboratory of Luminescent Materials and Devices (South China University of Technology). L.S. acknowledges the National Science Foundation (Partnerships for Research and Education in Materials, DMR-1205670), Air Force Office of Scientific Research (No. FA9550-12-1-0159), and a Faculty Large Grant from the University of Connecticut for partial support of this project.

References

1. I. Etchart, I. Hernández, A. Huignard, M. Bérard, W. P. Gillin, R. J. Curry and A. K. Cheetham, *Journal of Materials Chemistry*, 2011, **21**, 1387-1394.
2. G. Kumar, M. Pokhrel and D. Sardar, *Materials Letters*, 2012, **68**, 395-398.
3. C. Yuan, G. Chen, P. N. Prasad, T. Y. Ohulchanskyy, Z. Ning, H. Tian, L. Sun and H. Ågren, *Journal of Materials Chemistry*, 2012, **22**, 16709-16713.
4. A. Shooshtari, P. Meshkinfam, T. Touam, M. P. Andrews and S. I. Najafi, *Optical Engineering*, 1998, **37**, 1188-1192.
5. P. M. Peters, D. S. Funk, A. P. Peskin, D. L. Veasey, N. A. Sanford, S. N. Houde-Walter and J. S. Hayden, *Applied Optics*, 1999, **38**, 6879.
6. Z. Wang, Y. Wang, Y. Li and H. Zhang, *Journal of Materials Research*, 2011, **26**, 693-696.
7. M. Chong, K. Pita and C. Kam, *Applied Physics A*, 2004, **79**, 433.
8. J. Li, Y. Wang and B. Liu, *Journal of Luminescence*, 2010, **130**, 981.
9. Q. Yu, H. Zeng, Z. Liu, J. Ren, G. Chen, Z. Wang and L. Sun, *Journal of Alloys and Compounds*, 2014, **590**, 92-95.
10. N. Sonoyama, K. Kawamura, A. Yamada and R. Kanno, *Journal of Luminescence*, 2008, **128**, 1679-1683.
11. G. Gasparotto, S. A. M. Lima, M. R. Davolos, J. A. Varela, E. Longo and M. A. Zaghete, *Journal of Luminescence*, 2008, **128**, 1606-1610.
12. C. Liu, Y. Wang, Y. Hu, R. Chen and F. Liao, *Journal of Alloys and Compounds*, 2009, **470**, 473-476.

13. Y. Hu, W. Zhuang, H. Ye, S. Zhang, Y. Fang and X. Huang, *Journal of Luminescence*, 2005, **111**, 139-145.

14. S. Ye, Y.-j. Li, D.-c. Yu, G.-p. Dong and Q.-Y. Zhang, *Journal of Materials Chemistry*, 2011, **21**, 3735-3739.

15. B. M. van der Ende, L. Aarts and A. Meijerink, *Physical Chemistry Chemical Physics*, 2009, **11**, 11081-11095.

16. R. Martín-Rodríguez, R. Valiente and M. Bettinelli, *Applied Physics Letters*, 2009, **95**, 091913.

17. R. Martín-Rodríguez, R. Valiente, F. Rodríguez, F. Piccinelli, A. Speghini and M. Bettinelli, *Physical Review B*, 2010, **82**, 075117.

18. J. Suyver, A. Aebischer, D. Biner, P. Gerner, J. Grimm, S. Heer, K. Krämer, C. Reinhard and H. Güdel, *Optical Materials*, 2005, **27**, 1111-1130.

19. R. Bhargava, D. Gallagher, X. Hong and A. Nurmikko, *Physical Review Letters*, 1994, **72**, 416-419.

20. A. Morell and N. El Khiati, *Journal of The Electrochemical Society*, 1993, **140**, 2019-2022.

21. A. A. Bol and A. Meijerink, *The Journal of Physical Chemistry B*, 2001, **105**, 10203-10209.

22. T. Ohtake, N. Sonoyama and T. Sakata, *Chemical Physics Letters*, 1998, **298**, 395-399.

23. G. Tian, Z. Gu, L. Zhou, W. Yin, X. Liu, L. Yan, S. Jin, W. Ren, G. Xing and S. Li, *Advanced Materials*, 2012, **24**, 1226-1231.

24. H. Zeng, Q. Yu, Z. Wang, L. Sun, J. Ren, G. Chen and J. Qiu, *Journal of the American Ceramic Society*, 2013, **96**, 2476-2480.

25. G. Blasse and A. Bril, *Philips technical review*, 1970, **31**, 304-334.

26. Z. P. Li, B. Dong, Y. Y. He, B. S. Cao and Z. Q. Feng, *Journal of Luminescence*, 2012, **132**, 1646-1648.

27. G. F. J. Garlick and C. L. Richards, *Journal of Luminescence*, 1974, **9**, 432-439.

28. X. Wu, H. Zeng, Q. Yu, C. Fan, J. Ren, S. Yuan and L. Sun, *RSC Advances*, 2012, **2**, 9660-9664.

29. M. Raukas, K. C. Mishra, C. Peters, P. C. Schmidt, K. H. Johnson, J. Choi and U. Happek, *Journal of Luminescence*, 2000, **87–89**, 980-982.

30. Z. Wang, Y. Wang, Y. Li and B. Liu, *Journal of The Electrochemical Society*, 2010, **157**, J125-J129.

31. H. Yang, P. G. Kotula, Y. Sato, M. Chi, Y. Ikuhara and N. D. Browning, *Materials Research Letters*, 2014, **2**, 16-22.

32. J. Iqbal, X. Liu, A. Majid, D. Yu and R. Yu, *Europhysics Letters*, 2009, **87**, 57004.

33. Z. Wang, Y. Wang, Y. Li and B. Liu, *Journal of Alloys and Compounds*, 2011, **509**, 343-346.

34. C. Zhang and J. Lin, *Chemical Society Reviews*, 2012, **41**, 7938-7961.

35. Y. Li, Z. Wang, L. Sun, Z. Wang, S. Wang, X. Liu and Y. Wang, *Materials Research Bulletin*, 2014, **50**, 36-41.

36. Q. Yan, Y. Liu, G. Chen, N. Da and L. Wondraczek, *Journal of the American Ceramic Society*, 2011, **94**, 660-662.

37. E. Chukova, Anti-Stokes Luminescence and Its Potential Applications), Moscow: Sovetskoe Radio1980.

38. Y. Tanabe and S. Sugano, *Journal of the Physical Society of Japan*, 1954, **9**, 766-779.

39. G. Tian, Z. Gu, L. Zhou, W. Yin, X. Liu, L. Yan, S. Jin, W. Ren, G. Xing, S. Li and Y. Zhao, *Advanced Materials*, 2012, **24**, 1226-1231.

40. M. Kawano, H. Takebe and M. Kuwabara, *Optical Materials*, 2009, **32**, 277-280.

41. J. Flores, G. Caldino, A. Hernández, G. Camarillo, B. Cabrera, H. Del Castillo, A. Speghini, M. Bettinelli and S. Murrieta, *physica status solidi (c)*, 2007, **4**, 922-925.